



Anomalous Couplings Project

Progress Report and documentation of Tools

Annik Olbrechts

Started 4 April 2014
Version: March 12, 2015



Contents

1	Pending issues	1
2	Used Tools and Techniques	3
3	Generator level bottlenecks	5
4	Transfer Functions	7
5	Preliminary Results	9
6	Understanding MadWeight Results	11
7	Analyzing FeynRules model	13
8	MadGraph/MadWeight issues	15
9	Event Selection	17
10	Event corrections and reconstruction	19
11	Theory link with partial widths	21
11.1	Partial width of top-quark decay	22
11.2	Simplification in limit-cases	23
11.2.1	Only 1 coupling non-zero	23
11.2.2	Massless b-limit	23
11.2.3	Only 1 coupling non-zero within the massless b-limit	25
11.3	Understanding symmetric behavior	26

Chapter 1

Pending issues

- Does this created FeynRules model still contain Effective Field Theory?
- If the kinematics doesn't change for coupling parameters larger than 1, how is it than possible to differentiate the different configurations which will be studied?
- Understand *CorrectPhi* comment in MadWeight name
→ Maybe related with phi issues of neutrino's ...
- EventWeight calculated in analyzer should be integrated into MadWeight output (Should MadWeight weight just be multiplied with the EventWeight for each event?)
Otherwise all the effort to include JES and PU has no influence at all.
- Update EventNumberInformation file to only count the information when the event has passed the eventSelection requirements. Otherwise just discard this event from the output file in order to avoid a long .txt file and long running time ...
- Construct nTuple in such a way that the likelihood and weight distributions can be calculated for specific p_T cuts without having to run the entire base code again. So perhaps also necessary to include some of the different python scripts which have been created. Hence avoid spending too much time on improving them.
- Need to understand how MadWeight deals with the permutations ... Should this permutation of the light jets be done within MadWeight or should two .lhco files be created and sent separately to MadWeight. If the latter is the case, how should they be combined afterwards ?
- Specific MadWeight question for the latest version:
*The 'refine' option allows you to realunch the computation of the weights which have a precision lower than X. **But how can you find this precision?***
- Should a ScaleFactor correction be applied for the Branching ratio ?
This is not the case in code of James, but should find recommendations somewhere.
- **To Check:** Does MadWeight give a different weight when the Neutrino Mass changes?
→ Currently mass is manually set to zero ...
- Check whether the created root file can be trusted when the number of considered b-tags is greater than 1 ... *Why this comment??*

Chapter 2

Used Tools and Techniques

Chapter 3

Generator level bottlenecks

Chapter 4

Transfer Functions

Chapter 5

Preliminary Results

Chapter 6

Understanding MadWeight Results

Chapter 7

Analyzing FeynRules model

Chapter 8

MadGraph/MadWeight issues

Chapter 9

Event Selection

Chapter 10

Event corrections and reconstruction

Chapter 11

Theory link with partial widths

11.1 Partial width of top-quark decay

The partial width of the top-quark decay can be expressed in terms of the anomalous couplings in the Wtb interaction as represented in the following equations.

The first and less extensive one describes the longitudinal decay.

$$\begin{aligned} \Gamma_0 = & \frac{g^2 |\vec{q}|}{32\pi} \left\{ \frac{m_t^2}{m_W^2} \left[|V_L|^2 + |V_R|^2 \right] (1 - x_W^2 - 2x_b^2 - x_W^2 x_b^2 + x_b^4) - 4x_b \text{Re} V_L V_R^* \right. \\ & + \left[|g_L|^2 + |g_R|^2 \right] (1 - x_W^2 + x_b^2) - 4x_b \text{Re} g_L g_R^* \\ & - 2 \frac{m_t}{m_W} \text{Re} [V_L g_R^* + V_R g_L^*] (1 - x_W^2 - x_b^2) \\ & \left. + 2 \frac{m_t}{m_W} x_b \text{Re} [V_L g_L^* + V_R g_R^*] (1 + x_W^2 - x_b^2) \right\} \end{aligned} \quad (11.1)$$

with:

$$x_W = \frac{m_W}{m_t} \quad (11.2a)$$

$$x_b = \frac{m_b}{m_t} \quad (11.2b)$$

$$|\vec{q}| = \frac{1}{2m_t} \sqrt{m_t^4 + m_W^4 + m_b^4 - 2m_t^2 m_W^2 - 2m_t^2 m_b^2 - 2m_W^2 m_b^2} \quad (11.2c)$$

A similar equation can also be formulated for the left- and right-handed top-quark decay, which only differ partially with a minus sign. The right-handed part corresponds to the plus-sign option while the left-handed contribution contains the minus-sign.

$$\begin{aligned} \Gamma_{R,L} = & \frac{g^2 |\vec{q}|}{32\pi} \left\{ \frac{m_t^2}{m_W^2} \left[|V_L|^2 + |V_R|^2 \right] (1 - x_W^2 + x_b^2) - 4x_b \text{Re} V_L V_R^* \right. \\ & + \frac{m_t^2}{m_W^2} \left[|g_L|^2 + |g_R|^2 \right] (1 - x_W^2 - 2x_b^2 - x_W^2 x_b^2 + x_b^4) - 4x_b \text{Re} g_L g_R^* \\ & - 2 \frac{m_t}{m_W} \text{Re} [V_L g_R^* + V_R g_L^*] (1 - x_W^2 - x_b^2) \\ & + 2 \frac{m_t}{m_W} x_b \text{Re} [V_L g_L^* + V_R g_R^*] (1 + x_W^2 - x_b^2) \Big\} \\ & \pm \frac{g^2}{64\pi} \frac{m_t^3}{m_W^2} \left\{ -x_W^2 \left[|V_L|^2 - |V_R|^2 + |g_L|^2 - |g_R|^2 \right] (1 - x_b^2) \right. \\ & + 2x_W \text{Re} [V_L g_R^* + V_R g_L^*] + 2x_W x_b \text{Re} [V_L g_L^* + V_R g_R^*] \Big\} \\ & \times (1 - 2x_W^2 - 2x_b^2 + x_W^4 - 2x_W^2 x_b^2 + x_b^4) \end{aligned} \quad (11.3)$$

In order to transform these partial width formulas into helicity fractions, also the total width of the top quark decay is needed. This because each helicity fraction is defined as the corresponding partial width divided by the total width.

$$\begin{aligned} \Gamma = & \frac{g^2 |\vec{q}|}{32\pi} \frac{m_t^2}{m_W^2} \left\{ \left[|V_L|^2 + |V_R|^2 \right] (1 + x_W^2 - 2x_b^2 - 2x_W^4 + x_W^2 x_b^2 + x_b^4) - 4x_b \text{Re} V_L V_R^* \right. \\ & - 12x_W^2 x_b \text{Re} V_L V_R^* + 2 \left[|g_L|^2 + |g_R|^2 \right] \left(1 - \frac{x_W^2}{2} - 2x_b^2 - \frac{x_W^4}{2} - \frac{x_W^2 x_b^2}{2} + x_b^4 \right) \\ & - 12x_W^2 x_b \text{Re} g_L g_R^* - 6x_W \text{Re} [V_L g_R^* + V_R g_L^*] (1 - x_W^2 - x_b^2) \\ & \left. + 6x_W x_b \text{Re} [V_L g_L^* + V_R g_R^*] (1 + x_W^2 - x_b^2) \right\} \end{aligned} \quad (11.4)$$

11.2 Simplification in limit-cases

11.2.1 Only 1 coupling non-zero

If we consider the case where only the V_L coupling parameter is non-zero, the above definitions get reduced to the following formulas.

$$\Gamma_0 = \frac{g^2 |\vec{q}| m_t^2}{32\pi m_W^2} |V_L|^2 (1 - x_W^2 - 2x_b^2 - x_W^2 x_b^2 + x_b^4) \quad (11.5)$$

$$\Gamma_{R,L} = \frac{g^2 |\vec{q}|}{32\pi} |V_L|^2 (1 - x_W^2 + x_b^2) \pm \frac{g^2 m_t^3}{64\pi m_W^2} \{-x_W^2 |V_L|^2 (1 - x_b^2)\} \quad (11.6)$$

$$\Gamma = \frac{g^2 |\vec{q}| m_t^2}{32\pi m_W^2} |V_L|^2 (1 + x_W^2 - 2x_b^2 - 2x_W^4 + x_W^2 x_b^2) \quad (11.7)$$

So this implies that the helicity fractions can be defined as follows:

$$F_0 = \frac{\Gamma_0}{\Gamma} = \frac{(1 - x_W^2 - 2x_b^2 - x_W^2 x_b^2 + x_b^4)}{(1 + x_W^2 - 2x_b^2 - 2x_W^4 + x_W^2 x_b^2)} \quad (11.8)$$

$$F_{R,L} = \frac{\Gamma_{R,L}}{\Gamma} = \frac{m_W^2}{m_t^2} \frac{(1 - x_W^2 + x_b^2)}{(1 + x_W^2 - 2x_b^2 - 2x_W^4 + x_W^2 x_b^2)} \pm \frac{m_t}{2|\vec{q}|} \frac{-x_W^2 (1 - x_b^2)}{(1 + x_W^2 - 2x_b^2 - 2x_W^4 + x_W^2 x_b^2)} \quad (11.9)$$

From the above two equations can easily be concluded that in cases where only one of the Wtb-coupling coefficients is non-zero, there will be no influence visible on the helicity fractions. This because no interference between different coupling coefficients occurs which allows the cancellation of this single coupling coefficient. This behavior is indeed retrieved in the different $\cos \theta^*$ distributions which have been studied in detail. The ones with only one coupling constant active can be found in Figure 11.1.

It is important to note that the same is also true when only the real and imaginary part of one coupling are varied. In those cases there is also no interference between different coupling constants which is necessary in order to introduce a different between the partial widths and the total width. For example when considering only the left-handed vector coupling, the only term which remains in the width definitions is $|V_L|^2 = \text{Re}(V_L)^2 + \text{Im}(V_L)^2$. However since it does not matter whether this term consists of both the real and the imaginary part or only the real part, it will cancel out when dividing the partial width part by the total width. This behavior is indeed retrieved in the $\cos \theta^*$ distributions, as can be seen in Figure 11.2.

11.2.2 Massless b-limit

Within the Wtb interaction the mass of the bottom quark is almost negligible compared to the massive W-boson and the top quark. Hence it is rather standard to use a so-called massless b-limit when considering the Wtb interaction, an approach which also explains the suppression of the right-handed helicity fraction of the W-boson.

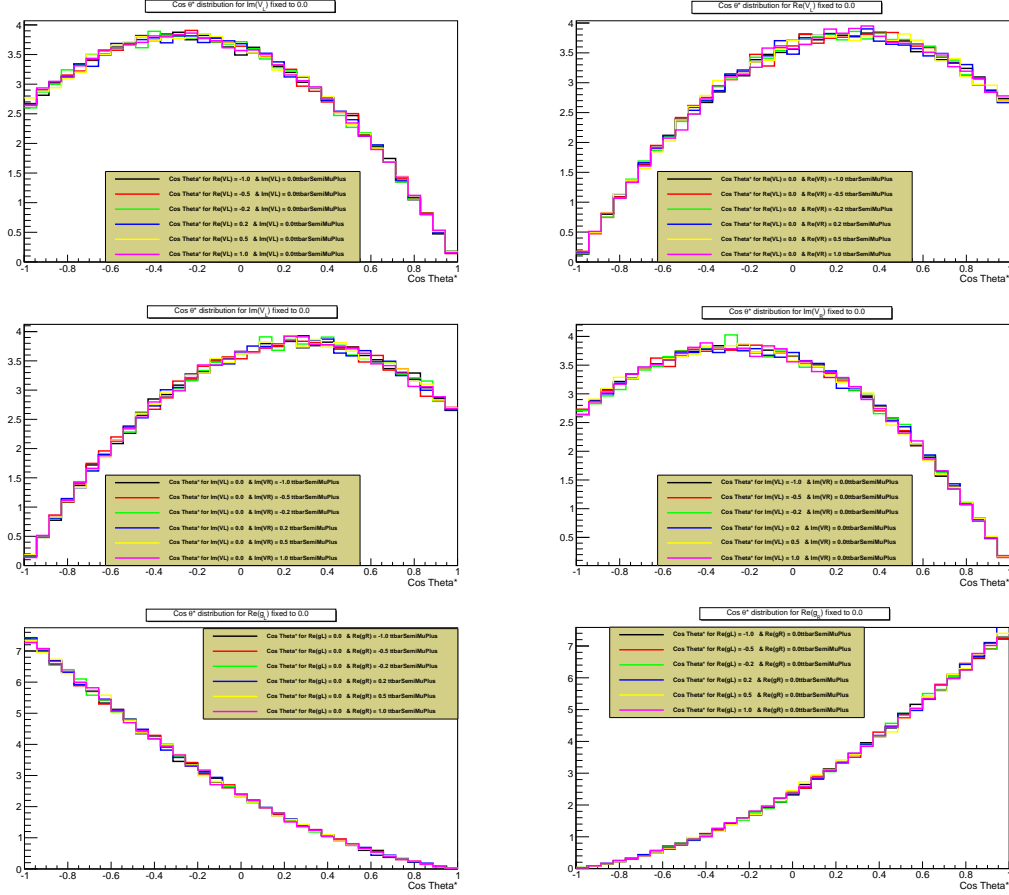


Figure 11.1: Distributions of $\cos \theta^*$ for configurations where only one of the Wtb -coupling coefficients is non-zero while the other one is varied between -1 and 1 . The two upper distributions show the case when only the real part of the two vector couplings is non-zero while the two middle ones represent the case when only their imaginary part is non-zero. Finally the two lower distributions give the $\cos \theta^*$ distribution for the real part of the tensor couplings. The same conclusion holds for all distributions shown here, namely that no shape difference occurs when only one of the couplings is non-zero as was indicated by the formulas given above.

When applying this assumption, the partial and total width formulas can be simplified significantly as will be shown in the following equations since the terms containing x_b can be neglected. For simplicity only the real parts of the vector couplings are considered, but the same is true for other combinations.

$$\Gamma_0 = \frac{g^2 |\vec{q}| m_t^2}{32\pi m_W^2} [|V_L|^2 + |V_R|^2] (1 - x_W^2) \quad (11.10)$$

$$\begin{aligned} \Gamma_{R,L} = & \frac{g^2 |\vec{q}| m_t^2}{32\pi m_W^2} [|V_L|^2 + |V_R|^2] (1 - x_W^2) \\ & \pm \frac{g^2}{64\pi m_W^2} \frac{m_t^3}{m_W^2} \left\{ -x_W^2 [|V_L|^2 - |V_R|^2] \right\} (1 - 2x_W^2 + x_W^4) \end{aligned} \quad (11.11)$$

$$\Gamma = \frac{g^2 |\vec{q}| m_t^2}{32\pi m_W^2} [|V_L|^2 + |V_R|^2] (1 + x_W^2 - 2x_W^4) \quad (11.12)$$

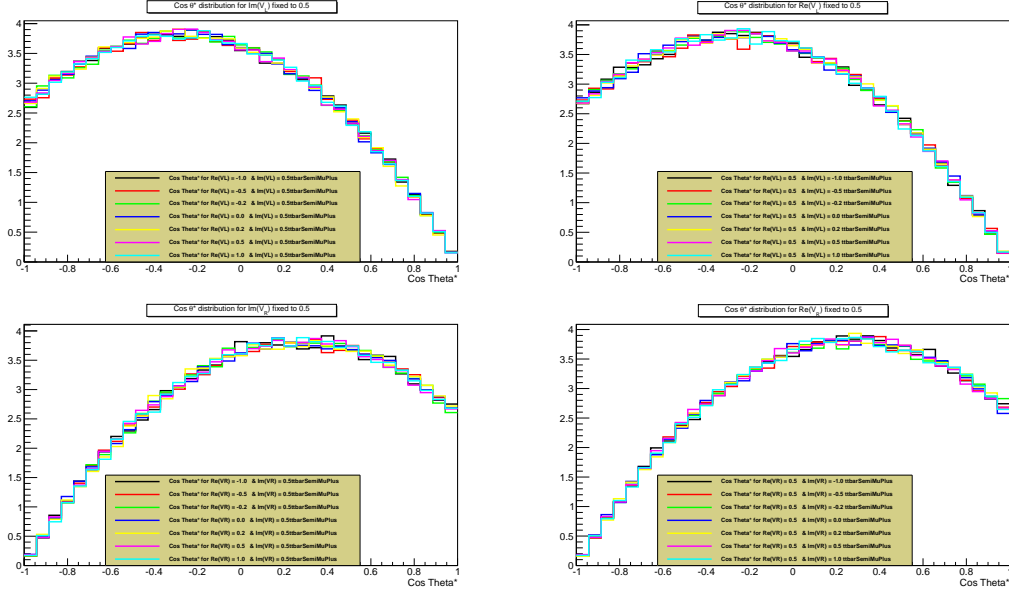


Figure 11.2

From this can be seen that the longitudinal helicity fraction is not influenced at all when working in the massless b-limit. The right-handed and left-handed helicity fractions, on the other hand, have an opposite coupling-coefficient dependent part. This is again clearly visible in the studied $\cos \theta^*$ distributions, which all behave similar around $\cos \theta^* = 0$. This is shown in Figure 11.3.

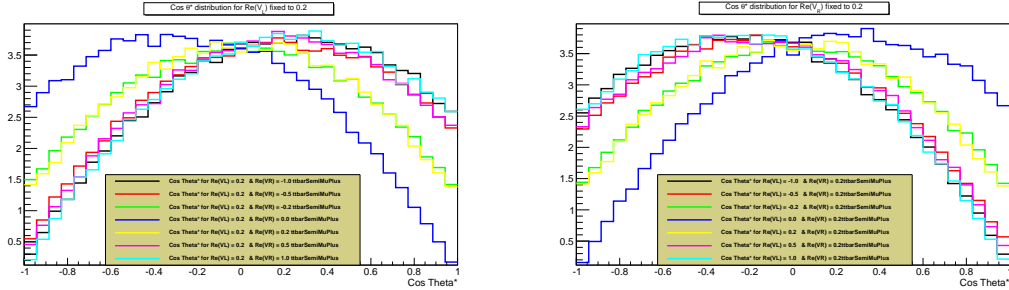


Figure 11.3: ...

11.2.3 Only 1 coupling non-zero within the massless b-limit

The equations defined when considering only 1 non-zero coupling, Equations (11.8) and (11.14), can be simplified even further when assuming the massless b-limit.

$$F_0 = \frac{(1 - x_W^2 - 2x_b^2 - x_W^2 x_b^2 + x_b^4)}{(1 + x_W^2 - 2x_b^2 - 2x_W^4 + x_W^2 x_b^2)} \quad (11.13)$$

$$F_{R,L} = \frac{m_W^2}{m_t^2} \frac{(1 - x_W^2 + x_b^2)}{(1 + x_W^2 - 2x_b^2 - 2x_W^4 + x_W^2 x_b^2)} \pm \frac{m_t}{2|\vec{q}|} \frac{-x_W^2(1 - x_b^2)}{(1 + x_W^2 - 2x_b^2 - 2x_W^4 + x_W^2 x_b^2)} \quad (11.14)$$

For the simplified case where only 1 of the couplings is varied the dependency on the top quark mass can be calculated explicitly by using Equations (11.2). Applying these definitions changes Equations (11.8) and (11.14) as follows¹:

$$\begin{aligned}
F_0 &= \frac{1 - x_W^2 - 2x_b^2 - x_W^2 x_b^2 + x_b^4}{1 + x_W^2 - 2x_b^2 - 2x_W^4 + x_W^2 x_b^2} \\
&= \frac{1 - \frac{m_W^2}{m_t^2} - 2\frac{m_b^2}{m_t^2} - \frac{m_W^2}{m_t^2} \frac{m_b^2}{m_t^2} + \frac{m_b^4}{m_t^4}}{1 + \frac{m_W^2}{m_t^2} - 2\frac{m_b^2}{m_t^2} - 2\frac{m_W^4}{m_t^2} + \frac{m_W^2}{m_t^2} \frac{m_b^2}{m_t^2}} \\
&= \frac{m_t^4}{m_t^4} \frac{m_t^4 - m_W^2 m_t^2 - 2m_b^2 m_t^2 - m_W^2 m_b^2 + m_b^4}{1 + m_W^2 m_t^2 - 2m_b^2 m_t^2 - 2m_W^4 + m_W^2 m_b^2 + m_b^4} \\
&\stackrel{\approx_{m_b=0}}{\approx} \frac{m_t^4 - m_W^2 m_t^2}{m_t^4 + m_W^2 m_t^2 - 2m_W^4} \\
\\
F_{R,L} &= \frac{m_W^2}{m_t^2} \frac{1 - x_W^2 + x_b^2}{1 + x_W^2 - 2x_b^2 - 2x_W^4 + x_W^2 x_b^2} \pm \frac{m_t}{2|\vec{q}|} \frac{-x_W^2(1 - 2x_W^2 - 2x_b^2 + x_W^4 - 2x_W^2 x_b^2 + x_b^4)}{1 + x_W^2 - 2x_b^2 - 2x_W^4 + x_W^2 x_b^2} \\
&= \frac{m_t^4}{m_t^4} \left\{ \frac{m_W^2}{m_t^2} \frac{1 - m_W^2 m_t^2 + m_b^2 m_t^2}{1 + m_W^2 m_t^2 - 2m_b^2 m_t^2 - 2m_W^4 + m_W^2 m_b^2} \right. \\
&\quad \left. \pm \frac{m_t}{2|\vec{q}|} \frac{-m_W^2}{m_t^2} \frac{m_t^4 - 2m_W^2 m_t^2 - 2m_b^2 m_t^2 + m_W^4 - 2m_W^2 m_b^2 + m_b^4}{m_t^4 + m_W^2 m_t^2 - 2m_b^2 m_t^2 - 2m_W^4 + m_W^2 m_b^2} \right\} \\
&\approx \frac{m_W^2}{m_t^2} \frac{m_t^4 - m_W^2 m_t^2}{1 + m_W^2 m_t^2 - 2m_W^4} \pm \frac{m_t}{2|\vec{q}|} \frac{-m_W^2}{m_t^2} \frac{m_t^4 - 2m_W^2 m_t^2 + m_W^4}{m_t^4 + m_W^2 m_t^2 - 2m_W^4} \\
&\approx \frac{m_W^2}{m_t^2} \frac{m_t^2(m_t^2 - m_W^2)}{m_t^4 + m_W^2 m_t^2 - 2m_W^4} \pm \frac{2m_t^2}{2(m_t^2 - m_W^2)} \frac{-m_W^2}{m_t^2} \frac{(m_t^2 - m_W^2)^2}{m_t^4 + m_W^2 m_t^2 - 2m_W^4} \\
&\approx m_W^2 \left(\frac{m_t^2 - m_W^2}{m_t^4 + m_W^2 m_t^2 - 2m_W^4} \right) \mp m_W^2 \left(\frac{m_t^2 - m_W^2}{m_t^4 + m_W^2 m_t^2 - 2m_W^4} \right) \\
&= \begin{cases} 0 & \text{for right-handed helicity fraction} \\ 2m_W^2 \frac{m_t^2 - m_W^2}{m_t^4 + m_W^2 m_t^2 - 2m_W^4} & \text{for left-handed helicity fraction} \end{cases}
\end{aligned}$$

Hence when creating the $\cos \theta^*$ distribution for different top-quark masses it is expected to see a clear shape difference for the left-handed helicity fraction. As postulated by the Standard Model, no right-handed contribution is expected and from the above equation is clear that this contribution does not depend on the considered top-quark mass. Again this can be seen on the $\cos \theta^*$ distributions when varying the top quark mass between 153 GeV and 193 GeV in steps of 10 GeV, as shown in Figure 11.4.

11.3 Understanding symmetric behavior

While studying all the different $\cos \theta^*$ distributions for all the considered configurations, there was one peculiar observation. Every studied $\cos \theta^*$ distribution clearly showed a symmetric relationship between the negative and positive part of each coupling coefficient. Again this can be explained using the partial top quark width definitions given above

¹This because within this massless b-limit $|\vec{q}|$ can be simplified to $\frac{m_t^2 - m_W^2}{2m_t}$.

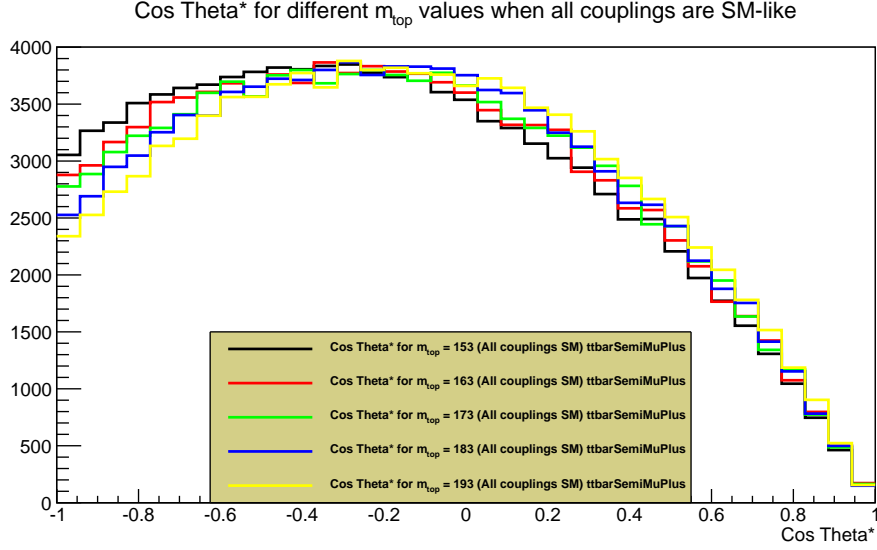


Figure 11.4: Distribution of $\cos \theta^*$ when varying the top quark mass.

since with these equations it is possible to track down the term which depends on the sign of the coefficient.

The only terms which need to know the sign of the considered coefficient are the mixing terms such as $ReV_L V_R^*$ for example. However most of these mixing terms, and all of the most straightforward ones, are scaled with a factor x_b implying that they are negligible in the massless b-limit. So mixing the vector and tensor couplings should give less symmetric $\cos \theta^*$ distributions than the current studied mixings between vector and tensor couplings separately.

Figure 11.5 clearly shows that the symmetric behavior is caused by low mass of the bottom quark. Both distributions represent an identical configuration, with the only difference the bottom-quark mass.

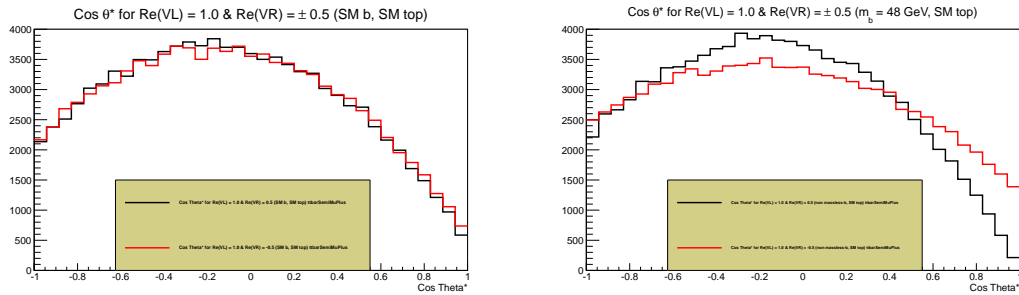


Figure 11.5: Influence of bottom-quark mass